JOURNAL OF THE AMERICAN COLLEGE OF CARDIOLOGY VOL. 72, NO. 13, 2018

PUBLISHED BY ELSEVIER

Alterations of Hyaluronan Metabolism in Acute Coronary Syndrome

Implications for Plaque Erosion

Daniela Pedicino, MD, PhD,[a,b,*] Ramona Vinci, PhD,[a,b,*] Ada F. Giglio, MD,[a,b] Eugenia Pisano, PhD,[a,b] Italo Porto, MD, PhD,[a,b] Rocco Vergallo, MD, PhD,[a,b] Giulio Russo, MD, PhD,[a,b] Aureliano Ruggio, MD,[a,b] Alessia D'Aiello, MD,[a,b] Davide Flego, PhD,[a,b] Gianmarco Annibali, MD,[a,b] Francesco Trotta, MD,[a,b] Roberto Piacentini, PhD,[c] Giampaolo Niccoli, MD, PhD,[a,b] Giovanna Liuzzo, MD, PhD,[a,b,†] Filippo Crea, MD[a,b,†]

ABSTRACT

BACKGROUND Superficial erosion currently causes at least one-third of acute coronary syndromes (ACS), and its incidence is increasing. Yet, the underlying mechanisms in humans are still largely unknown.

OBJECTIVES The authors sought to assess the role of hyaluronan (HA) metabolism in ACS.

METHODS Peripheral blood mononuclear cells were collected from ACS (n = 66), stable angina (SA) (n = 55), and control (CTRL) patients (n = 45). The authors evaluated: 1) gene expression of hyaluronidase 2 (HYAL2) (enzyme degrading high-molecular-weight HA to its proinflammatory 20-kDa isoform) and of CD44v1, CD44v4, and CD44v6 splicing variants of HA receptor; and 2) HYAL2 and CD44 protein expression. Moreover, they compared HYAL2 and CD44 gene expression in ACS patients with plaque erosion (intact fibrous cap and thrombus) and in ACS patients with plaque rupture, identified by optical coherence tomography analysis.

RESULTS Gene expression of HYAL2, CD44v1, and CD44v6 were significantly higher in ACS as compared with SA ($p = 0.003$, $p < 0.001$, and $p = 0.033$, respectively) and CTRL subjects ($p < 0.001$, $p < 0.001$, and $p = 0.009$, respectively). HYAL2 protein expression was significantly higher in ACS than in SA ($p = 0.017$) and CTRL ($p = 0.032$), whereas no differences were found in CD44 protein expression. HYAL2 and CD44v6 gene expression was significantly higher in patients with plaque erosion than in those with plaque rupture ($p = 0.015$ and $p = 0.029$, respectively).

CONCLUSIONS HYAL2 and CD44v6 splicing variants seem to play an important role in ACS, in particular when associated with plaque erosion. After further validation, HYAL2 might represent a potentially useful biomarker for the noninvasive identification of this mechanism of coronary instability. (J Am Coll Cardiol 2018;72:1490–503)

The causes of acute coronary syndromes (ACS) are multiple and incompletely understood (1,2). A sizable proportion of patients presenting with ACS has obstructive atherosclerosis and systemic evidence of inflammation, supporting the hypothesis that an inflammatory outburst may lead to plaque rupture with thrombosis (3–5). However, >40% of patients with ACS have low levels of systemic markers of inflammation (6), suggesting that other mechanisms play a pathogenic role (1,7). In particular, in the era of statin treatment, we are facing a gradual shift in the histological features of unstable plaque, from rupture to erosion (8,9).

Plaque erosion is associated with ACS in at least one-third of patients, and it is characterized by thrombus formation at the site of a

Listen to this manuscript's audio summary by *JACC* Editor-in-Chief Dr. Valentin Fuster.

From the [a]Department of Cardiovascular and Thoracic Sciences, Catholic University of the Sacred Heart, Rome, Italy; [b]Fondazione Policlinico Universitario A. Gemelli, IRCCS, Rome, Italy; and the [c]Institute of Human Physiology, Catholic University of the Sacred Heart, IRCCS-Fondazione Policlinico Universitario A. Gemelli, Rome, Italy. *Drs. Pedicino and Vinci contributed equally to this work as first authors. †Drs. Liuzzo and Crea contributed equally to this work as senior authors. This work was supported by the Catholic University of the Sacred Heart, Rome, Italy (R4124500458 LINEA D.1 2016) and IRCCS-Fondazione Policlinico Universitario "A. Gemelli." The authors have reported that they have no relationships relevant to the contents of this paper to disclose.

Manuscript received May 2, 2018; revised manuscript received June 14, 2018, accepted June 25, 2018.

ISSN 0735-1097/$36.00 https://doi.org/10.1016/j.jacc.2018.06.072

de-endothelialized atherosclerotic plaque. The in vivo detection of eroded plaques is based on optical coherence tomography (OCT) assessment, which shows coronary thrombosis in the absence of plaque rupture (10–13). Previous histological studies documented intense immunostaining positivity for hyaluronan (HA) and its receptor CD44 along the interface between the endothelium and luminal thrombus in eroded plaque, and abundance of myeloperoxidase (MPO)-positive cells within the overlying thrombus (14). Accordingly, ACS patients with plaque erosion on OCT exhibit higher MPO levels in peripheral blood as compared with those showing plaque rupture (15). Moreover, coculture of polymorphonuclear leukocytes (PMNs) with endothelial cells induces endothelial injury and apoptosis, at least in part mediated by toll-like receptor-2 (TLR2) activation and flow perturbation (8,16,17). Of note, HA is an endogenous activator for TLR2 (18). Systematic OCT studies documented a higher prevalence of plaque erosion associated with non-ST-segment elevation ACS (about 60%), as compared with ST-segment elevation myocardial infarction (STEMI) that conversely shows a prevalence of plaque rupture around 70% (19,20). The higher prevalence of eroded plaques occurs in women under 50 years of age and in current smokers, whereas other coronary risk factors such as diabetes, hypertension, dyslipidemia, and chronic kidney disease are less common. Furthermore, plaque erosion frequently involves the left anterior descending coronary artery and coronary bifurcations, probably due to local flow perturbation (21,22).

SEE PAGE 1504

HA is one of the major constituents of the extracellular matrix and, under physiological condition, consists of a large glycosaminoglycan chain that undergoes fragmentation during infection and tissue damage. At homeostasis, extracellular HA is found predominantly in its high-molecular-weight form (HMW-HA) of over 1,000 kDa, and its production by stromal cells is balanced by its cellular uptake and degradation (23). During local inflammation, HA fragments of low molecular weight (LMW-HA) accumulate extracellularly and propagate the inflammatory response, whereas the restoration of HMW-HA is associated with the resolution of the inflammatory burst (24). Interestingly, fragments derived from HA metabolism are involved in PMN recruitment and activation (25,26).

CD44 is the major cell-surface HA binding protein (27,28). It is a polymorphic type I transmembrane glycoprotein encoded by a single gene, but expressed in over 20 isoforms as a result of cell-specific glycosylation and alternative splicing of at least 10 variable exons. The expression of variant isoforms is mostly detectable in hemopoietic cells, particularly in peripheral blood mononuclear cells (PBMCs) and in lymph nodes (29). Under homeostatic conditions, immune cells barely bind HA. Activation of immune cells induces HA binding by CD44 in a process that is usually accompanied by an increase in CD44 expression. Most of the functions ascribed to CD44 can be attributed to its ability to bind and internalize HA (30,31).

Cellular HA synthases (HAS-1, -2, and -3) and hyaluronidases (HYAL1, -2, -3, and 4, PH-20, and HYALP1) mediate the turnover of HA (32). During inflammation, an increase in HA is paralleled by a decrease in chain length (below 500 kDa), possibly due to modulation of HAS and HYAL activities (33) or to cleavage induced by locally released reactive oxygen and nitrogen species (34). The cellular uptake of HA, mostly mediated by macrophages, stems from CD44-HA binding and partial degradation by HYAL2 on the cell surface, with subsequent internalization (28,35). The HYAL2 enzyme hydrolyzes HMW-HA to intermediate-sized HA fragments of approximately 20 kDa, which are further hydrolyzed to small oligosaccharides by other hyaluronidases (mainly HYAL1). Interestingly, both HYAL1 and HYAL2 contribute to catabolism of HA in a CD44-dependent manner (36). Recent studies showed that HYAL2 protein expression on endothelial cells depends at least in part from shear stress and that low shear stress-induced endothelial impairment is partly mediated by increased HYAL2 activity (37). Moreover, by the analysis of carotid specimens of patients undergoing endarterectomy, a correlation has been found between plaque instability and both HYAL2 activity and CD44v3 (a splicing variant of CD44) expression (38).

In this study, we sought to investigate the role of HA, HYAL2, and CD44 in the pathogenesis of ACS and their possible implications for plaque erosion.

METHODS

The Online Appendix includes a detailed description of patient characteristics and methods. We enrolled 3 groups of patients: 1) 66 patients with a first diagnosis of ACS, admitted to our coronary care unit with non-STEMI; 2) 55 chronic stable angina (SA) patients; and 3) 45 control patients (CTRL) without overt coronary

ABBREVIATIONS AND ACRONYMS

ACS = acute coronary syndrome
ANOVA = analysis of variance
CTRL = control patients
HA = hyaluronan
HMW-HA = high-molecular-weight hyaluronan
IFC = intact fibrous cap
IQR = interquartile range
LMW-HA = low-molecular-weight hyaluronan
LPS = lipopolysaccharide
MFI = mean fluorescence index
MPO = myeloperoxidase
OCT = optical coherence tomography
PBMC = peripheral blood mononuclear cell
PMN = polimorphonuclear leukocyte
RFC = ruptured fibrous cap
RT-qPCR = real-time-quantitative polymerase chain reaction
SA = stable angina
STEMI = ST-segment elevation myocardial infarction

FIGURE 1 Patient Flow-Chart

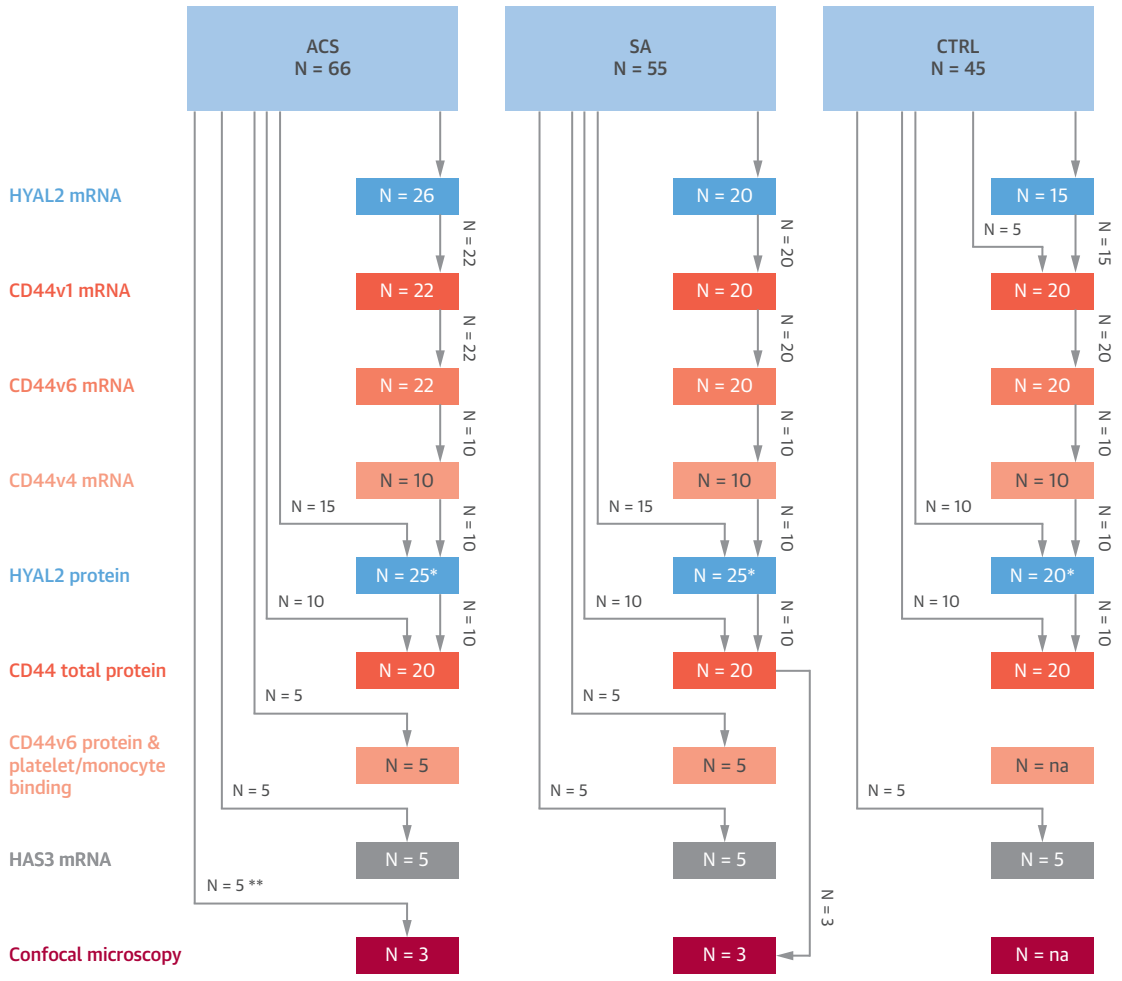

Flow chart showing patient allocation in each experiment. *10 patients, of 25, were tested before and after stimulation with LMW-HA, HMA-HA, and LPS; for 5 patients, a different antibody was used for the HYAL2 flow-cytometric assay. **2 of 5 samples were used for the confocal microscopy experimental set-up. ACS = acute coronary syndrome; CTRL = control; ECM = extracellular matrix; EC = endothelial cell; HA = hyaluronan; HC = control; HMW-HA = high-molecular-weight hyaluronan; HYAL2 = hyaluronidase 2; LMW-HA = low-molecular-weight hyaluronan; LPS = lipopolysaccharide; N = number; na = not available; SA = stable angina.

artery disease screened in our out-patients clinic for cardiovascular prevention (Figure 1).

Cellular and molecular analyses were performed on isolated PBMCs, under basal condition and after 16 h of incubation with HMW-HA, LMW-HA (R&D Systems by Lifecore Biomedical, Chaska, Minnesota) and with *Escherichia coli* lipopolysaccharide (LPS) (Sigma-Aldrich, St. Louis, Missouri), as positive control. The following parameters were then assessed before and after stimulation: 1) mRNA expression of HYAL2 (26 ACS, 20 SA, and 15 CTRL) by real-time-quantitative polymerase chain reaction (RT-qPCR); 2) mRNA expression of 3 different CD44 splicing variants, CD44v1 and CD44v6 (22 ACS, 20 SA, and 20 CTRL), and CD44v4 (10 for each group) by RT-qPCR; 3) HYAL2 (25 ACS, 25 SA, and 20 CTRL) and total CD44 (20 for each group) protein expression before and after stimulation (10 for each group) on monocytes by flow cytometry; 4) CD44v6 basal protein expression in ACS and SA (5 for each group); 5) platelet-monocyte binding by flow cytometry in 5 ACS and 5 SA patients, after 16 h of coincubation, with and without LMW-HA stimulation; and 6) moreover, HYAL2 and CD44 protein colocalization, before and after stimulation, was analyzed by confocal immunofluorescence microscopy in ACS and SA patients (3 for each group). Finally, in 15 of 66 ACS patients who underwent OCT analysis of culprit coronary

plaques before stent implantation, it was possible to clearly identify the feature of the culprit plaques as plaque erosion characterized by an intact fibrous cap (IFC) with thrombus (6 patients) or plaque rupture containing a large necrotic core under a ruptured fibrous cap (RFC) (9 patients). We compared these 2 ACS subgroups for HYAL2 and CD44 alternative splicing variants gene expression. After a mean follow-up period of 12 ± 4 months, we reassessed 13 patients in order to investigate HYAL2 and CD44 gene expression over time.

STATISTICAL ANALYSIS. Continuous variables that were normally distributed as assessed by Shapiro Wilk test were described as mean ± SD. In this case, 1-way analysis of variance (ANOVA) and 1-ANOVA for repeated measures, with Bonferroni correction, were used for multiple comparisons. Data that did not follow a normal distribution were described as median and interquartile range (IQR), and they were analyzed by using a nonparametric test (the Kruskal-Wallis test and the Dunn's multiple pairwise comparisons for comparisons among groups, and the Friedman test for pairwise comparison within a group). Whenever the overall comparison between the 3 groups had a p value <0.01, we performed unpaired Student's *t*-test (for continuous variables that were normally distributed) or Mann-Whitney test (for nonparametric variables) to compare 2 groups, as appropriate. We used the nonparametric Spearman rank test for correlation analyses. For all the experimental assays performed, a 2-tailed p value ≤0.01 was considered statistically significant. Statistical analyses were performed with GraphPad Prism version 5.00 for Windows (GraphPad Software, La Jolla, California) and with SPSS software v22.0 (IBM, Armonk, New York).

RESULTS

Baseline characteristics of patient population are detailed in **Table 1**. The flow chart in **Figure 1** summarizes the patient enrollment for each experiment, and the Online Appendix includes additional figures.

EXPRESSION OF HYAL2 IN BASAL CONDITION AND AFTER STIMULATION WITH HMW-HA, LMW-HA, AND LPS. HYAL2 gene was overexpressed in unstimulated PBMCs of ACS patients (median 8.3; IQR: 10.2, relative expression) as compared to SA patients (median 4.9; IQR: 4.2) and CTRL (median 3.6; IQR: 5.0) (ANOVA for trend p = 0.0002; p = 0.003 and p = 0.0003 ACS vs. SA and CTRL, respectively) (**Figure 2A**). Online Figure 1 shows receiver-operating characteristic curves for HYAL2 gene expression.

After 16-h stimulation, HYAL2 gene expression was higher in ACS patients (median 16.9; IQR: 18.3, relative expression) as compared with SA patients (median 2.9; IQR: 2.0) and CTRL (median 2.7; IQR: 3.9) (ANOVA for trend p = 0.011; p = 0.045 and p = 0.048 ACS vs. SA and CTRL, respectively) for LMW-HA stimulation (**Figure 2B**). Interestingly, HYAL2 gene expression after stimulation with HMW-HA was similar in the 3 groups.

In keeping with the results of stimulation, at flow cytometry, unstimulated $CD14^+$ monocytes from ACS patients showed a higher HYAL2 protein expression (median mean fluorescence index [MFI] 2.2; IQR: 2.1) as compared with SA patients (median MFI 0.6; IQR: 1.1) and CTRL (median MFI 1.0; IQR: 0.8) (ANOVA for trend p = 0.002; p = 0.032 and p = 0.017 ACS vs. SA and CTRL, respectively) (**Figure 3A**). These data were further confirmed in 5 ACS and 5 SA samples by using a different HYAL2 polyclonal antibody for flow cytometry (p = 0.017) (Online Figure 2). After 16 h of stimulation, HYAL2 protein expression did not differ among groups (ANOVA for trend p = 0.02), although there was a significant increase in LPS-stimulated cells of ACS as compared with HMW-HA (**Figure 3B**).

In order to verify whether an increased HA catabolism in the basal condition was related also to an increased HA production, we tested the basal gene expression of hyaluronan synthase-3 (HAS3) in unstimulated PBMCs. No differences were observed among the groups (median for ACS 2.7; IQR: 1.6; for SA 2.2; IQR: 2.3; for CTRL 4.8; IQR: 2.6; ANOVA for trend p = 0.05) (Online Appendix, Online Figure 3).

Finally, we analyzed serum levels of soluble HYAL2 by enzyme-linked immunosorbent assay. No differences were observed among the 3 groups (ANOVA for trend p = 0.79) (Online Figure 4).

GENE EXPRESSION OF HYAL2 AND CARDIOVASCULAR RISK FACTORS: ROLE OF CIGARETTE SMOKING. Among the patients tested for HYAL2 gene expression, HYAL-2 was significantly higher in smoker ACS patients (n = 10) (median 33.1; IQR: 44.9) compared with nonsmoker ACS patients (n = 16) (median 7.5; IQR: 4.0; p = 0.0004), to smoker SA patients (n = 7) (median 7.0; IQR: 7.8; p = 0.001) and smoker CTRL (n = 6) (median 5.2; IQR: 3.5; p = 0.03) (ANOVA for trend p = 0.001) (**Figure 4A**). HYAL2 protein expression showed a similar behavior (median MFI for smoker ACS 3.4; IQR: 1.7, for nonsmokers ACS 1.1; IQR: 1.0; for smoker SA 0.9; IQR: 0.9; for smoker CTRL 0.7; IQR: 0.6; ANOVA for trend 0.008) (**Figure 4B**). After revising other common cardiovascular risk factors

TABLE 1 Baseline Characteristics of the Study Population

	CTRL (n = 45)	SA (n = 55)	ACS (n = 66)	p Value
Demographic characteristics				
Age, yrs	62 ± 13	70 ± 9	65 ± 12	0.12
Sex, male/female	23/22	36/19	40/26	0.34
BMI, kg/m^2	25 ± 4	27 ± 4	28 ± 5	0.13
Time of blood sampling from symptoms onset, h	NA	NA	9 ± 3.4	NA
Cardiovascular risk factors				
Hypertension	15 (33)	35 (63)	41 (62)	0.01*†
Dyslipidemia	9 (20)	30 (54)	34 (51)	0.01*†
Smoke	7 (15)	29 (52)	38 (57)	0.01*†
Family history of IHD	9 (20)	21 (38)	23 (35)	0.12
Obesity	7 (15)	12 (21)	19 (29)	0.26
Diabetes	4 (8)	22 (40)	21 (31)	0.01†‡
History				
Previous ACS	NA	4 (7)	7 (8)	0.09
Previous CABG	NA	1 (2)	5 (2)	0.38
Previous PCI	NA	2 (4)	3 (6)	0.08
Medications (at the time of blood sampling)				
Aspirin	9 (20)	38 (69)	41 (62)	0.01†‡
$P2Y_{12}$ receptor inhibitors	0 (0)	21 (38)	32 (48)	0.01†‡
ACE inhibitors	7 (15)	13 (23)	21 (31)	0.15
ARBs	4 (8)	15 (27)	12 (18)	0.01§
Calcium-channel blockers	0 (0)	9 (16)	9 (13)	0.02‡§
Statins	10 (22)	34 (61)	32 (48)	0.01*§
β-Blockers	8 (17)	29 (52)	26 (39)	0.01‡§
Diuretic agents	2 (4)	11 (20)	13 (20)	0.05‡§
Oral antidiabetic drugs	2 (4)	15 (27)	10 (15)	0.04†
Oral anticoagulant	0 (0)	4 (7)	6 (9)	0.13
Insulin	0 (0)	6 (11)	5 (7)	0.10
Laboratory assay				
cTnI >0.004 ng/ml	NA	NA	66 (100)	NA
Hemoglobin, g/dl	13 ± 1	13 ± 2	13 ± 3	0.85
Lymphocyte count, 10^9/l	2 ± 0.7	3 ± 1.7	2 ± 0.7	0.43
Platelets, 10^3/ml	183 ± 60	221 ± 60	220 ± 55	0.19
Glycemia, mg/dl	107 ± 21	116 ± 40	111 ± 31	0.82
Total cholesterol, mg/dl	162 ± 63	153 ± 42	174 ± 40	0.05
LDL, mg/dl	102 ± 38	96 ± 36	108 ± 33	0.05
HDL, mg/dl	61 ± 29	43 ± 13	39 ± 11	0.01*§
Triglycerides, mg/dl	111 ± 51	125 ± 52	151 ± 84	0.13
Creatinine, mg/dl	0.7 ± 0.1	0.92 ± 0.3	1.12 ± 0.4	0.09
ESR, mm/h	9 ± 8	14 ± 12	20 ± 11	0.22
hs-CRP, mg/l	0 (0–3)	4.4 (0.5–6.7)	13 (0.5–76.8)	<0.001†‖¶
In-hospital management				
Multivessel disease	NA	33 (60)	37 (56)	0.71
PCI for the index event	NA	32 (58)	45 (68)	0.26
CABG for the index event	NA	19 (34)	17 (25)	0.32
OMT without revascularization	NA	5 (7)	4 (6)	0.73
LVEF ≥50%	45 (100)	48 (87)	56 (84)	0.01‡

Values are mean ± SD, n, n (%), or median (interquartile range). Of note, ACS and SA patients have similar risk factor profile and medical treatment. *p < 0.01 ACS vs CTRL. †p < 0.01 SA vs CTRL. ‡p < 0.05 ACS vs CTRL. §p < 0.05 SA vs CTRL. ‖p < 0.01 ACS vs SA. ¶p < 0.001 ACS vs CTRL.

ACE = angiotensin-converting enzyme; ACS = acute coronary syndromes; ARBs = angiotensin II receptor blockers; BMI = body mass index; CABG = coronary artery bypass grafting; cTnI = cardiac troponin I; CTRL = control; ESR = erythrocyte sedimentation rate; HDL = high-density lipoprotein; hs-CRP = high-sensitivity C-reactive protein; IHD = ischemic heart disease; LDL = low-density lipoprotein; LVEF = left ventricular ejection fraction; NA = not available; OMT = optimal medical therapy; PCI = percutaneous coronary intervention; SA = stable angina.

FIGURE 2 **Gene Expression of HYAL2 in Basal Condition and After Stimulation**

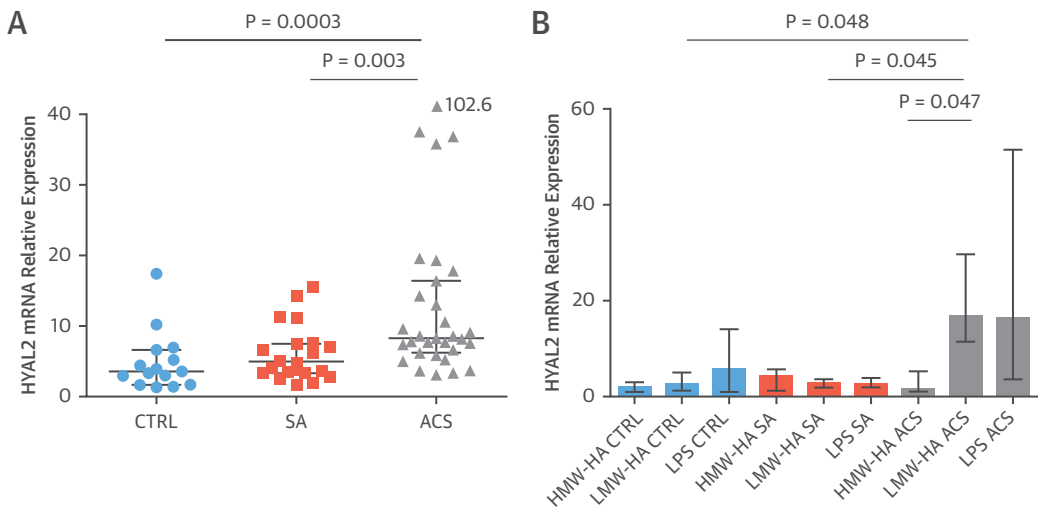

Graphs showing the gene expression of HYAL2 in PBMCs assessed by RT-qPCR (median ± IQR) in basal conditions (delta-threshold cycle [Δ-CT]) **(A)**, and after 16 h of incubation with the indicated treatments among the 3 groups **(B)**. IQR = interquartile range; PBMC = peripheral blood mononuclear cell; RT-qPCR = real-time–quantitative polymerase chain reaction; other abbreviations as in Figure 1.

among groups, HYAL2 gene expressions was not related to obesity, dyslipidemia, diabetes, or positive family history.

EXPRESSION OF CD44v1, CD44v6, AND CD44v4 ALTERNATIVE SPLICING VARIANTS IN BASAL CONDITIONS AND AFTER INCUBATION WITH LMW-HA, HMW-HA, AND LPS. We investigated gene expression of CD44 and transcript variants 1 (CD44v1), 6 (CD44v6), and 4 (CD44v4) in unstimulated PBMCs. CD44v1 gene expression was higher in ACS patients (median 29.5; IQR: 42.6, relative expression) compared with SA patients (median 4.2; IQR: 5.7) and CTRL (median 9.9; IQR: 6.0) (ANOVA for trend $p = 0.0003$; $p < 0.0001$ and $p = 0.0003$ ACS vs. SA and CTRL, respectively) (Figure 5A). CD44v6 gene expression also was significantly higher in ACS patients (median 12.4; IQR: 8.4, relative expression) as compared with SA patients (median 4.2; IQR: 12.5) and CTRL (median 7.7; IQR: 4.9) (ANOVA for trend $p = 0.009$; $p = 0.033$ and $p = 0.009$ ACS vs. SA and CTRL, respectively) (Figure 5B). In sharp contrast, CD44v4 gene expression was higher in SA patients (median 4.5 IQR: 3.4, relative expression) compared with both CTRL subjects (median 1.7; IQR: 0.8) and ACS patients (median 2.3; IQR: 1.9) (ANOVA for trend $p = 0.003$; $p = 0.005$ and $p = 0.043$ SA vs. CTRL and ACS, respectively) (Figure 5C). No significant differences were found for CD44v1, v6, and v4 splicing variants after 16-h stimulation with LMW-HA, HMW-HA, and LPS (Online Figure 5).

Of note, a positive correlation was observed between basal gene expression of HYAL2 and of CD44v6 in ACS patients ($r = 0.63$; $p = 0.016$) (Figure 5D), although no correlation was found between HYAL2 and CD44v1, and between HYAL2 and CD44v4 (Online Figure 6).

CD44 protein expression was assessed on the surface of $CD14^+$ monocytes by flow cytometry, using a CD44 antibody clone that recognizes an epitope common to the different isoforms of this molecule, in order to include in the analysis all the splicing variants. Moreover, in 5 ACS and in 5 SA patients a monoclonal antibody corresponding to the splicing variant 6 was tested. In basal conditions, no difference was found, neither in total CD44 protein expression comparing ACS (median MFI 35.1; IQR: 5.2) to SA patients (median 36.5; IQR: 8.6) and to CTRL (median 36.8; IQR: 7.3) (ANOVA for trend $p = 0.49$) (Figure 6A), nor in CD44v6 protein expression (Online Figure 7). After 16 h of stimulation, in ACS patients only, total CD44 protein expression was significantly increased in LPS-treated samples (MFI fold increase: median 1.17; IQR: 0.22) as compared with HMW-HA (median 0.96; IQR: 0.08) and LMW-HA (median 0.94; IQR: 0.08; ANOVA for trend $p = 0.001$; $p = 0.004$ and $p = 0.009$ LPS vs. HMW-HA and LMW-HA, respectively) (Figure 6B). After revising all the common cardiovascular risk factors among groups, CD44

FIGURE 3 Protein Expression of HYAL2 in Basal Condition and After Stimulation

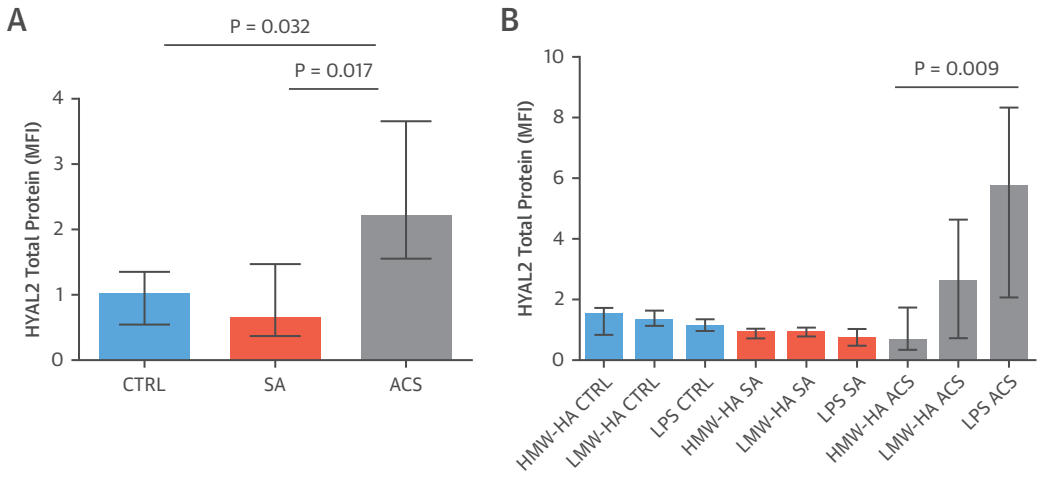

Graphs showing the protein expression of HYAL2 on $CD14^{+}$ monocytes assessed by flow-cytometry (MFI) (median ± IQR), in basal conditions **(A)** and after 16 h of incubation with the indicated treatments among the 3 groups. Data are presented as fold changes as compared with untreated samples **(B)**. CTRL = control subjects; MFI = mean fluorescence index; other abbreviations as in Figures 1 and 2.

splicing variant gene expressions were not related to smoking (Online Figure 8), obesity, dyslipidemia, diabetes, or family history.

Online Figure 1 shows receiver-operating characteristic curves for CD44v1 and CD44v6 gene expression.

EFFECT OF HA ON PLATELET–MONOCYTE BINDING IN ACS. We compared platelet-monocyte binding (expressed as % of CD14/CD42b-positive cells) by flow cytometry in 5 ACS and 5 SA patients after 16 h of coincubation, with and without LMW-HA stimulation. Despite the low number of patients, our data

FIGURE 4 Gene and Protein Expression of HYAL2 and Smoking Habits

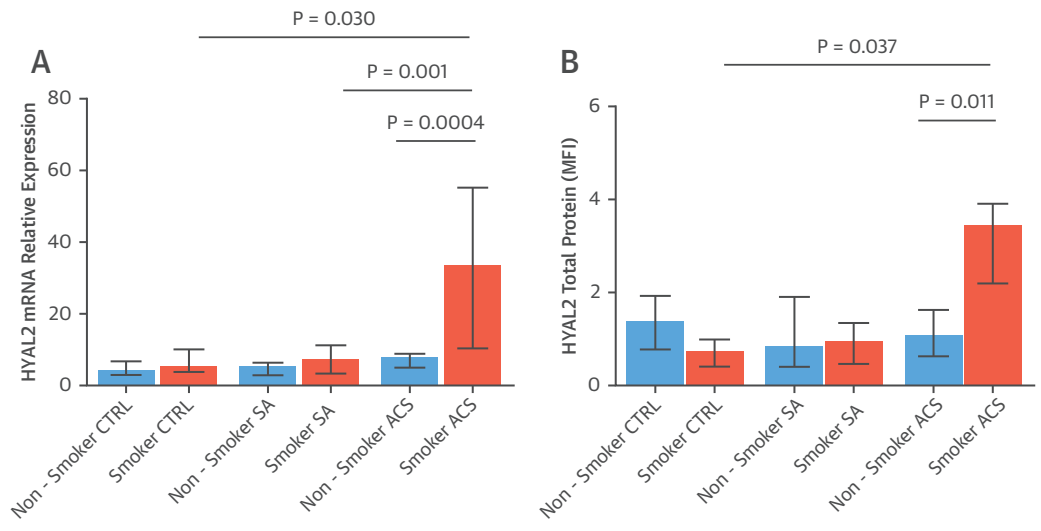

Graphs showing gene (Δ-CT) **(A)** and protein (MFI) **(B)** expression of HYAL2 on unstimulated PBMCs according to smoking habits, as assessed by RT-qPCR and flow cytometry, respectively (median ± IQR). Abbreviations as in Figures 1, 2, and 3.

FIGURE 5 **CD44 Splicing Variant Gene Expression**

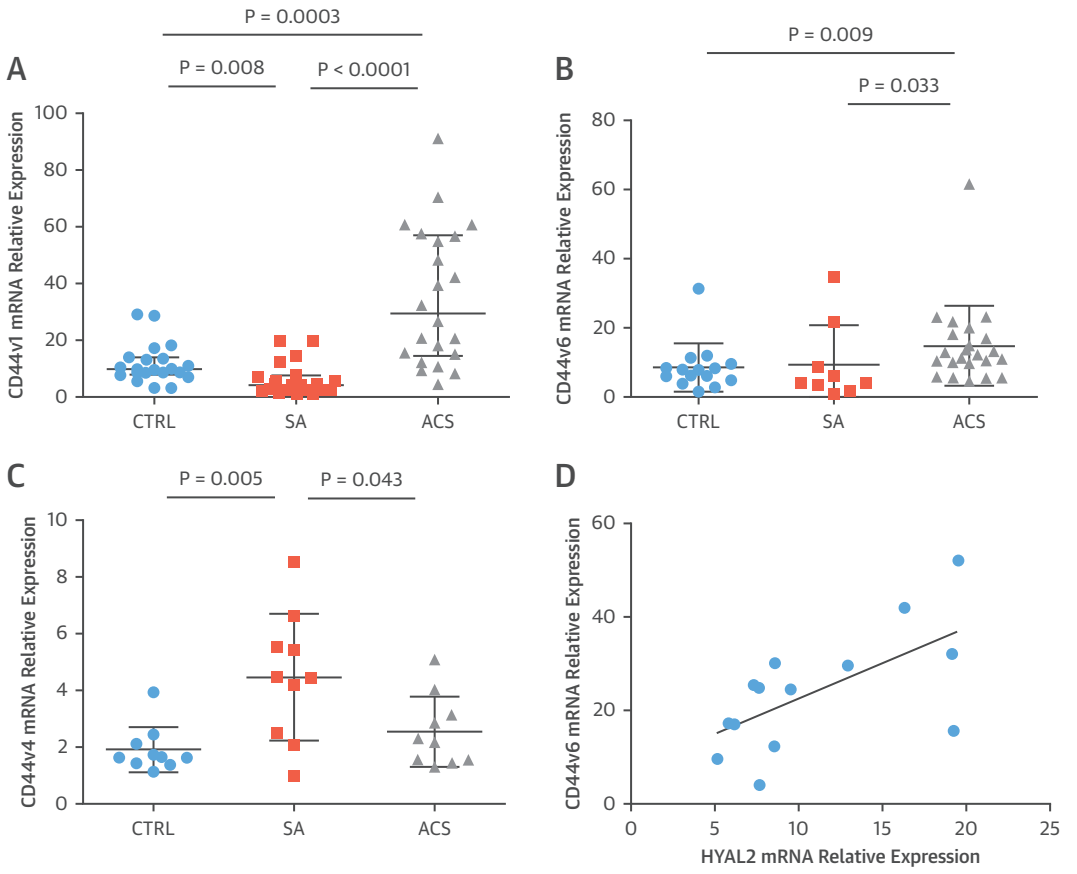

Graphs showing the gene expression of CD44v1 **(A),** CD44v6 **(B)**, and CD44v4 **(C)** on unstimulated PBMCs assessed by RT-qPCR (median ± IQR) (Δ-CT). **(D)** Correlation between HYAL2 and CD44v6 gene expression on unstimulated PBMCs of ACS patients. Abbreviations as in **Figures 1, 2, and 3**.

showed an increase in platelet-monocyte binding after LMW-HA treatment in patients presenting with ACS (median MFI fold increase 31.42; IQR: 31.08) as compared with SA (median 3.0; IQR: 3.19) (**Figure 7**). On confocal microscopy analyses, we found a trend of increased CD44 and HYAL2 protein expression in ACS patients after stimulation (Online Figure 9). Interestingly, although CD44 and HYAL2 colocalized on cell membranes in SA patients also after stimulation, in ACS, this colocalization was lost, thus suggesting an intense alteration of the CD44/HYAL2 pathway due to a failure of synergism (**Figure 8**).

HYAL2, CD44v6, AND CD44v1 GENE EXPRESSION ACCORDING TO OCT ANALYSIS OF THE UNSTABLE PLAQUES: ACUTE PHASE AND FOLLOW-UP. HYAL2 and CD44v6 gene expression were significantly higher in ACS patients with plaque erosion (IFC group) as compared with those with plaque rupture (RFC group) (for HYAL2: median 15.2; IQR: 17.6 vs. median 7.3; IQR: 4.9; $p = 0.015$; for CD44v6: median 17.5; IQR: 35.3 vs. median 11.0; IQR: 2.3; $p = 0.029$) (**Figures 9A and 9B**). In sharp contrast, CD44v1 gene expression was higher in RFC group as compared with the IFC group (for CD44v1: median 48.6; IQR: 59.5 vs. median 10.2; IQR: 5.5; $p = 0.029$) (**Figure 9C**).

Of note, after 12 ± 4 months of follow-up in which all patients received similar pharmacological treatments, HYAL2 and CD44v6 gene expression dramatically decreased in patients with plaque erosion (IFC group) as compared with the same patients analyzed during the acute phase, with expression levels becoming similar to those observed in the RFC group. Thus, in the IFC patient subset, median HYAL2 expression was 2.0; IQR: 0.7 at follow-up ($p = 0.004$; follow-up vs. baseline). In the same IFC patient

FIGURE 6 CD44 Protein in Basal Conditions and After Stimulation

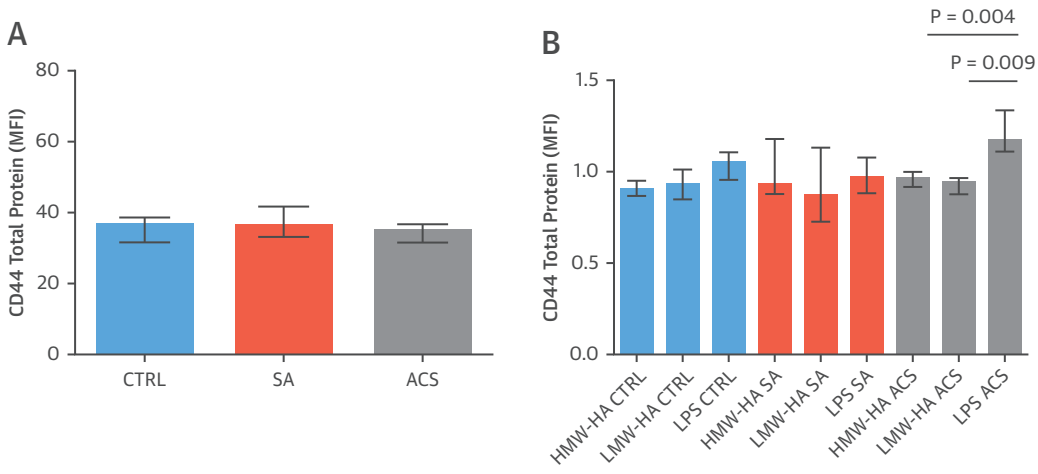

Protein expression of CD44 on $CD14^+$ monocytes assessed by flow cytometry (MFI) (median ± IQR), in basal conditions **(A)** and after 16 h of incubation with the indicated treatments **(B),** among the 3 groups. In **B**, data are presented as fold changes as compared with untreated samples. Abbreviations as in Figures 1 to 3.

subset, median CD44v6 expression was 5.2; IQR: 1.6 at follow-up (p = 0.004 follow-up vs. baseline) (**Figures 9A and 9B**). Similarly, a significant decrease over time was observed for CD44v1 gene expression in patients with plaque rupture (RFC median 2.8; IQR: 2.2; p = 0.016 follow-up vs. baseline) (**Figure 9C**). See also Online Table 1 for raw data and Online Figure 10.

Finally, even though the number of patients examined was very small, and we could not perform any statistical analysis, we found the highest HYAL2 gene expression in smoker ACS patients with IFC on OCT (Online Figure 11).

FIGURE 7 Effect of HA on Platelet/Monocyte Binding

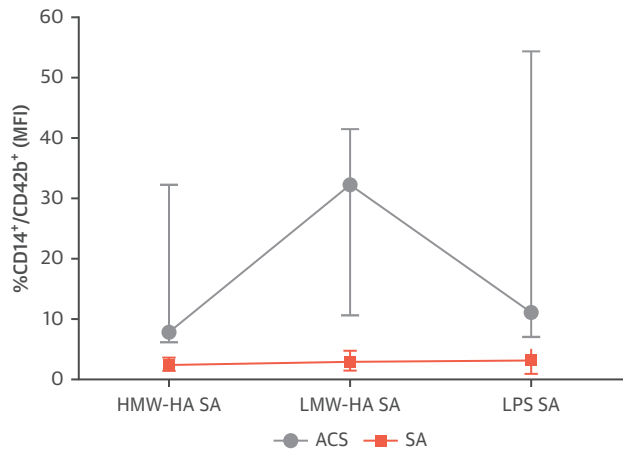

Graph showing platelet–monocyte binding (expressed as % of CD14/CD42b-positive cells) in ACS as compared with SA patients after 16 h of incubation with the indicated treatments. Data are presented as fold changes as compared with untreated samples. HA = hyaluronan; other abbreviations as in Figures 1, 2, and 3.

DISCUSSION

Plaque erosion is associated with ACS in at least one-third of patients. Recent studies documented a higher prevalence of plaque erosion in non-STEMI, in women under 50 years of age, and in current smokers (21,22). Experimental studies proposed an exciting model of plaque instability associated with erosion, where blood flow perturbation determines endothelial activation by HA-induced TLR2 stimulation leading to de-endothelialization, PMN recruitment and thrombus formation (8,9,16). These data, together with the notion of an intense immunostaining for CD44 on eroded plaques and for MPO on the overlying thrombus at histological examination of coronary lesions of sudden coronary death victims, led to the intriguing hypothesis that the accumulation of HA along the plaque may be involved, through CD44 receptor engagement, in this pathogenic mechanism of ACS (10,13,14). Adjunctive experimental evidence recently highlighted the role of HYAL2 as a possible mediator of endothelial dysfunction in the presence of perturbed flow (8,37).

FIGURE 8 HYAL2 and CD44 Protein Colocalization at Confocal Microscopy

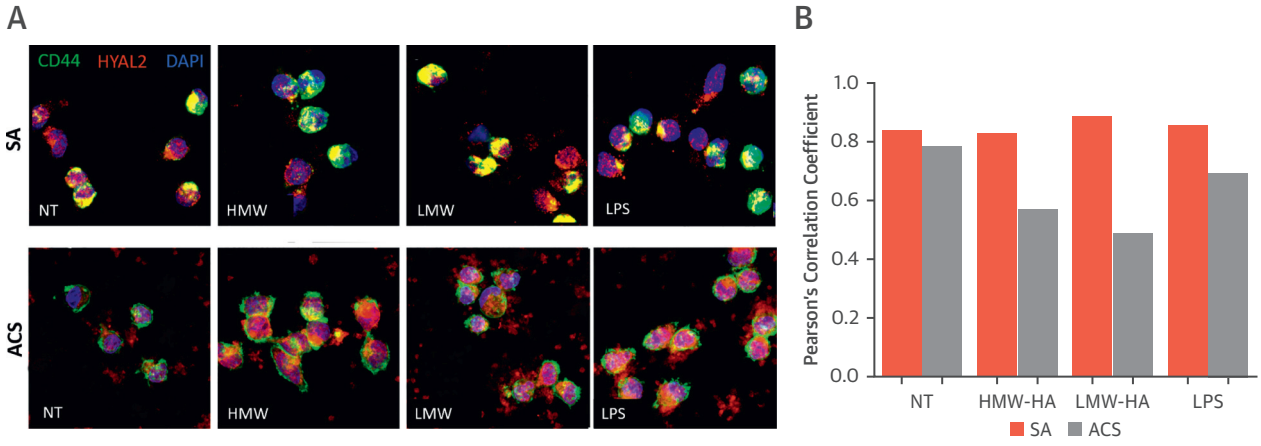

(A) Representative confocal images of CD44 **(green)** and HYAL2 **(red)** protein expression, for SA and ACS samples in different incubation conditions (NT, HMW-HA, LMW-HA, and LPS, respectively). DAPI **(blue)** indicates nuclei. The **yellow** fluorescence indicates colocalization of CD44 and HYAL2. **(B)** Colocalization (yellow fluorescence) of HYAL2 and CD44 in 3 ACS and 3 SA patients. Confocal images (at a resolution of 512 × 512 pixels) of a minimum of 50 cells for each condition were analyzed by NIS-Elements imaging software. Semiquantification of the degree of colocalization obtained using pixel-intensity correlation (Pearson's correlation coefficient: maximum of colocalization = 1). Of note, colocalization does not necessarily mean physical interaction between the 2 molecules CD44 and HYAL2. HMW = high molecular weight; LMW = low molecular weight; NT = not treated; other abbreviations as in Figure 1.

This enzyme might be involved also in the generation of a local inflammatory response, given its ability to cut HMW-HA in proinflammatory fragments of 20 kDa, that are involved inter alia in PMN chemotaxis and activation (25).

HYAL2 EXPRESSION IN ACS: ROLE OF HA PATHWAY IN PLAQUE EROSION. In our study, for the first time in the clinical setting, we show an altered HA metabolism in ACS patients, characterized by enhanced HYAL2 gene expression in circulating PBMCs that is involved in the degradation of HMW-HA to 20-kDa LMW-HA fragments. Indeed, in ACS patients HYAL2 gene expression was significantly higher when compared with that observed in SA patients and in CTRL in the basal condition; furthermore, in ACS patients, but not in the 2 other groups, HYAL2 gene expression significantly increased after PBMC incubation with LMW-HA to levels that paralleled those observed with a potent proinflammatory stimulus (*E. coli* LPS). Enhanced HYAL2 expression was prevalent in patients presenting with ACS and OCT evidence of IFC. Of note, we found that HYAL2 gene expression was significantly enhanced in smoker versus nonsmoker ACS patients, whereas no difference was found between smokers and nonsmokers among SA patients and CTRL subjects. Even more interestingly, we found that smoker ACS patients presenting with IFC on OCT analysis had the highest HYAL2 gene expression and that also nonsmoker ACS patients with IFC showed higher levels than RFC (smokers or nonsmokers) (Online Appendix). Although these are very preliminary data, due to the small number of patients, they suggest hyper-reactivity to this environmental factor during the acute phase of coronary artery disease, in keeping with post mortem data suggesting that smoking is a risk factor for erosion (22).

In the general population, HYAL2 protein expression, assessed by flow-cytometry, paralleled what was observed for gene expression by RT-qPCR mRNA assessment.

CD44 RECEPTOR EXPRESSION IN ACS: DIFFERENTIAL EXPRESSION OF DIFFERENT SPLICING VARIANTS. Gene expression analysis of CD44 splicing variants revealed significantly higher levels of both CD44v1 and CD44v6 mRNA in ACS patients as compared with SA patients and CTRL subjects. Notably, patients with IFC showed higher gene expression of CD44v6, with a direct correlation between gene expression of this splicing variant and that of HYAL2. The differences observed in CD44v1, CD44v4, and CD44v6 gene expression between SA and ACS, and between IFC and RFC demonstrated that different isoforms of the CD44 receptor might be variously involved in different types of unstable

FIGURE 9 Gene Expression of HYAL2 and CD44 Splicing Variants According to OCT Analysis of the Unstable Plaques: Short-Term Phase and FUp

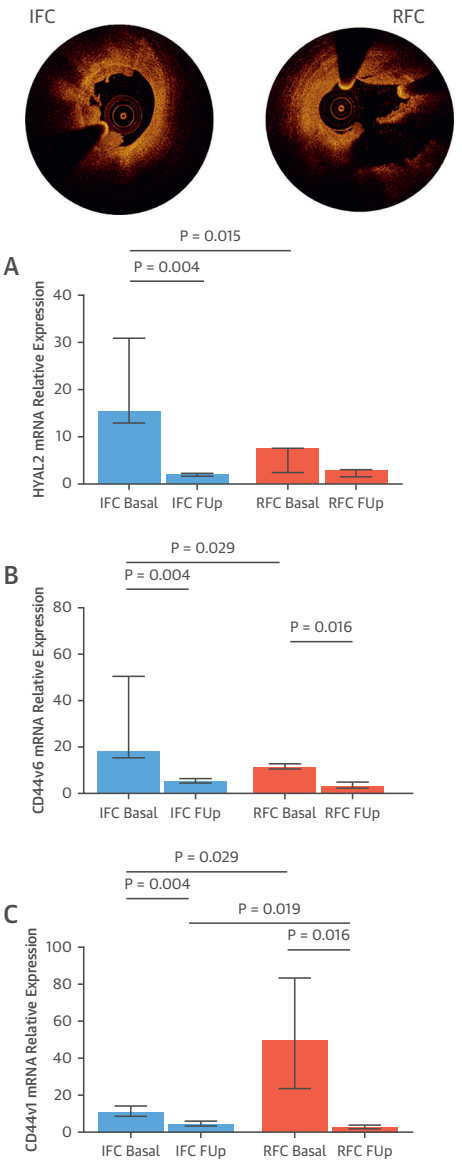

In the **upper part** of the figure, OCT representative images of IFC and RFC lesions. The **graphs** show gene expression of HYAL2 **(A)**, CD44v6 **(B),** and CD44v1 **(C)** in IFC and RFC ACS subgroups during the acute phase (basal) and after 1-year follow-up (FUp) assessed by RT-qPCR (median, IQR) (Δ-CT) FUp = follow up; IFC = intact fibrous cap; OCT = optical coherence tomography; RFC = ruptured fibrous cap; other abbreviations as in **Figures 1 and 2**.

plaques, with a specific commitment of CD44v6 in the HA metabolic pathway linked to plaque erosion. Of note, and in accord with our findings, previous experimental work has already documented a higher expression of other variants of CD44 receptor in unstable plaques (38). We did not find any difference in CD44 protein expression in circulating monocytes among ACS, SA, and CTRL under basal conditions. Yet, after incubation with LPS, CD44 protein levels increased in PBMCs from ACS patients, but not in those from SA patients, thus suggesting that enhanced CD44 gene expression translates into increased protein expression only under conditions of local inflammation, as might be the case in eroded plaques.

The data acquired at follow-up for both gene expression of HYAL2 and CD44 splicing variants documented a significant reduction of HYAL2 and CD44v6 expression in the IFC group and a significant reduction of CD44v1 for the RFC group, thus confirming that the alterations observed in our study were strictly limited to the acute phase of ACS (39,40).

Our data on CD44 splicing variants seem to suggest that what we observed in PBMCs might mirror what happens in endothelial cells at the site of the eroded plaque where enhanced expression of specific isoforms of the CD44 receptor might amplify HA-induced endothelial activation.

Taken together, these findings suggest that in plaque erosion, the enhanced expression of HYAL2 in PBMCs might provide a positive feedback promoting local LMW-HA formation, TLR2 stimulation, endothelial activation, and neutrophil accumulation, also enhanced by CD44 overexpression in neutrophils, eventually leading to thrombus formation. The latter might be also favored by LMW-HA accumulation resulting in enhanced monocyte-platelet binding (**Central Illustration**). This model derives from both the existing experimental and post-mortem studies on plaque erosion and the data emerging from our clinical study.

STUDY LIMITATIONS. First of all, our study was a prospective observational analysis that included a limited number of patients. No power calculation could be performed because of a lack of previous studies in this setting; thus, the enrollment of 66, 55, and 45 subjects for each group and their allocation in the different experiments performed were arbitrary, and they were mainly driven by the number of available PBMCs. Moreover, ACS and SA patients and controls were not properly matched for age, sex, and risk factors; however, no significant differences were observed in this regard between the ACS and SA groups, and none of these variables were independently associated with HYAL2 and CD44 expression on univariate analysis, with the exception of smoking

CENTRAL ILLUSTRATION **Altered Hyaluronan Pathway in Plaque erosion**

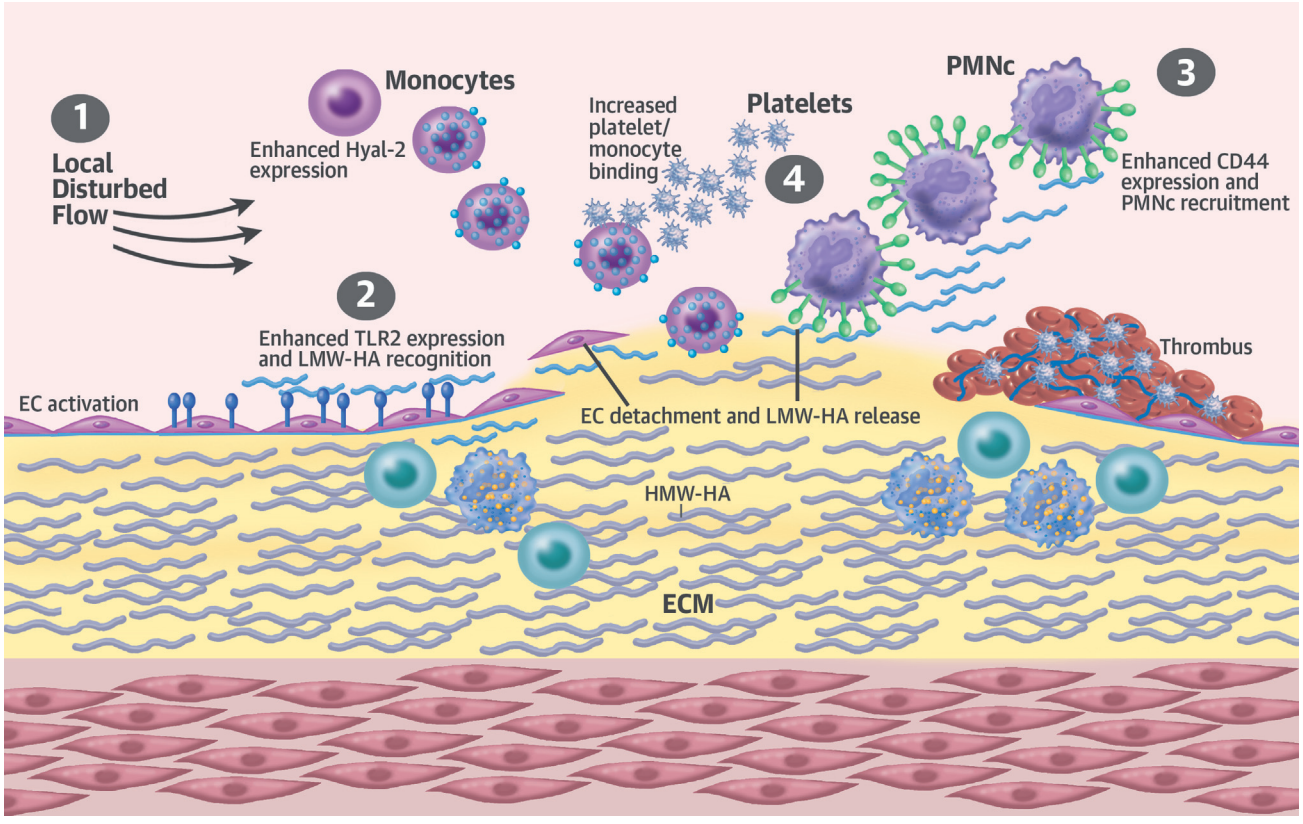

Pedicino, D. et al. J Am Coll Cardiol. 2018;72(13):1490–503.

Model of plaque erosion. The figure summarizes the driving hypothesis that derives from both the existing experimental and post-mortem studies on plaque erosion and the data emerging from this clinical study. Overexpression of HYAL2 in PBMCs (membrane, cytoplasm, and nuclei) under conditions of increased shear stress (#1) leads to degradation of HMW-HA to proinflammatory LMW-HA, which, in turn, promotes endothelial activation and detachment via TLR2 stimulation (#2), as well as neutrophil recruitment (#3), the latter being amplified by overexpression of CD44, which is necessary and sufficient for adhesion of neutrophils to LMW-HA. Finally, LMW-HA induces increased platelet-monocyte binding, thus promoting thrombus formation (#4). Scarcely represented inflammatory cells are found in the intima, close to the site of erosion (T-cells in **green** and foam cells). ECM = extracellular matrix; EC = endothelial cell; HA = hyaluronan; HMW-HA = high-molecular-weight hyaluronan; HYAL2 = hyaluronidase 2; LMW-HA = low-molecular-weight hyaluronan; PBMC = peripheral blood mononuclear cell; PMNc = polimorphonuclear cell.

and HYAL2 gene expression. These limitations imply 2 dominant methodological issues that cannot be eluded. First, several variables other than the coronary disease state might explain the differences observed across these 3 populations. Thus, we cannot exclude the likelihood that some of our findings of statistical significance might be false positives. Second, it is impossible in this type of study to determine a cause-effect relationship. More specifically, for obvious limitations, in this study, we analyzed PBMCs and we did not collect data on the molecular composition of the culprit plaque. Thus, we cannot say whether these alterations might have a causal role or whether they need to be considered as a consequence of the plaque fate. Finally, the greater limitation in our study is the lack of OCT imaging analysis for all the patients enrolled, because we obtained intracoronary imaging only for clinical reasons.

CONCLUSIONS

In our study, for the first time to our knowledge, we describe different molecular signatures in vivo in humans connecting a similar clinical presentation (ACS) with culprit plaques that show different

pathological features. This paves the way toward new immunomodulatory targets in ACS that might be of diagnostic and prognostic value by using specific biomarkers for a specific plaque phenotype, and that might be crucial in targeting new, personalized therapeutic approaches. Indeed, HA metabolism alteration could represent a novel therapeutic target in patients in whom ACS is caused by plaque erosion. More importantly, if confirmed in more robust and larger studies, HYAL2 might represent a noninvasive diagnostic tool allowing one to avoid the use of OCT imaging, which is quite expensive, time consuming, and burdened with risks. This might be even more valuable in centers in which OCT technology is not available, paving the path toward the noninvasive characterization of the mechanism of plaque instability in ACS patients (41).

ACKNOWLEDGMENTS The authors thank the catheterization laboratory director Prof. C. Trani and all the colleagues, technicians, and nurses for their technical and scientific support. The authors strongly believe in translational research involving clinicians, interventional cardiologists, and molecular biologists to promote personalized medicine.

ADDRESS FOR CORRESPONDENCE: Dr. Giovanna Liuzzo, Department of Cardiovascular and Thoracic Sciences, Catholic University of the Sacred Heart, Largo A. Gemelli, 1 - 00168, Rome, Italy. E-mail: giovanna.liuzzo@gmail.com.

PERSPECTIVES

COMPETENCY IN MEDICAL KNOWLEDGE: OCT studies of the pathogenesis of ACS have identified changes in unstable plaques that include but are not limited to rupture. Molecular pathways leading to plaque erosion involve alterations in metabolism of HA and its receptor, CD44, at the interface between the coronary endothelium and intraluminal thrombus.

TRANSLATIONAL OUTLOOK: In the future, assays for HA metabolites and detection of specific splicing variants of CD44 may allow for non-invasive identification of plaque erosion and guide diagnostic algorithms and targeted management strategies for patients with ACS.

REFERENCES

1. Crea F, Liuzzo G. Pathogenesis of acute coronary syndromes. J Am Coll Cardiol 2013;61:1–11.

2. Yeh RW, Sidney S, Chandra M, et al. Population trends in the incidence and outcomes of acute myocardial infarction. N Engl J Med 2010;362:2155–65.

3. Liuzzo G, Biasucci LM, Gallimore JR, et al. The prognostic value of C-reactive protein and serum amyloid a protein in severe unstable angina. N Engl J Med 1994;331:417–24.

4. Liuzzo G, Montone RA, Gabriele M, et al. Identification of unique adaptive immune system signature in acute coronary syndromes. Int J Cardiol 2013;168:564–7.

5. Libby P, Hansson GK. Inflammation and immunity in diseases of the arterial tree: players and layers. Circ Res 2015;116:307–11.

6. Cristell N, Cianflone D, Durante A, et al., FAMI Study Investigators. High-sensitivity C-reactive protein is within normal levels at the very onset of first ST-segment elevation acute myocardial infarction in 41% of cases: a multiethnic case-control study. J Am Coll Cardiol 2011;58:2654–61.

7. Crea F, Libby P. Acute coronary syndromes: the way forward from mechanisms to precision treatment. Circulation 2017;136:1155–66.

8. Franck G, Mawson T, Sausen G, et al. Flow perturbation mediates neutrophil recruitment and potentiates endothelial injury via TLR2 in mice: implications for superficial erosion. Circ Res 2017;121:31–42.

9. Bentzon JF, Falk E. Plaque erosion: new insights from the road less travelled. Circ Res 2017;121:8–10.

10. Virmani R, Kolodgie FD, Burke AP, Farb A, Schwartz SM. Lessons from sudden coronary death: a comprehensive morphological classification scheme for atherosclerotic lesions. Arterioscler Thromb Vasc Biol 2000;20:1262–75.

11. Niccoli G, Liuzzo G, Montone RA, Crea F. Advances in mechanisms, imaging and management of the unstable plaque. Atherosclerosis 2014;233:467–77.

12. Prati F, Uemura S, Souteyrand G, et al. OCT-based diagnosis and management of STEMI associated with intact fibrous cap. J Am Coll Cardiol Img 2013;6:283–7.

13. Jia H, Abtahian F, Aguirre AD, et al. In vivo diagnosis of plaque erosion and calcified nodule in patients with acute coronary syndrome by intravascular optical coherence tomography. J Am Coll Cardiol 2013;62:1748–58.

14. Kolodgie FD, Burke AP, Farb A, et al. Differential accumulation of proteoglycans and hyaluronan in culprit lesions: insights into plaque erosion. Arterioscler Thromb Vasc Biol 2002;22:1642e8.

15. Ferrante G, Nakano M, Prati F, et al. High levels of systemic myeloperoxidase are associated with coronary plaque erosion in patients with acute coronary syndromes: a clinicopathological study. Circulation 2010;122:2505–13.

16. Quillard T, Araujo HA, Franck G, Shvartz E, Sukhova G, Libby P. TLR2 and neutrophils potentiate endothelial stress, apoptosis and detachment: implications for superficial erosion. Eur Heart J 2015;36:1394–404.

17. Mullick AE, Soldau K, Kiosses WB, Bell TA III, Tobias PS, Curtiss LK. Increased endothelial expression of Toll-like receptor 2 at sites of disturbed blood flow exacerbates early atherogenic events. J Exp Med 2008;205:373–83.

18. Monslow J, Govindaraju P, Puré E. Hyaluronan: a functional and structural sweet spot in the tissue microenvironment. Front Immunol 2015;6:231.

19. Kubo T, Imanishi T, Takarada S, et al. Assessment of culprit lesion morphology in acute myocardial infarction. Ability of optical coherence tomography compared with intravascular ultrasound and coronary angioscopy. J Am Coll Cardiol 2007;50:933–9.

20. Chandran S, Watkins J, Abdul-Aziz A, et al. Inflammatory differences in plaque erosion and rupture in patients with ST-segment elevation myocardial infarction. J Am Heart Assoc 2017;6:e005868.

21. Dai J, Xing L, Jia H, et al. In vivo predictors of plaque erosion in patients with ST-segment elevation myocardial infarction: a clinical, angiographical, and intravascular optical coherence tomography study. Eur Heart J 2018;39:2077–85.

22. Jinnouchi H, Virmani R, Finn AV. Are characteristics of plaque erosion defined by

optical coherence tomography similar to true erosion in pathology? Eur Heart J 2018;39:2086–9.

23. Lee-Sayer SS, Dong Y, Arif AA, Olsson M, Brown KL, Johnson P. The where, when, how, and why of hyaluronan binding by immune cells. Front Immunol 2015;6:150.

24. Ferns GA, Konneh M, Rutherford C, Woolaghan E, Anggard EE. Hyaluronan (HYAL-BV 5200) inhibits neo-intimal macrophage influx after balloon-catheter induced injury in the cholesterol-fed rabbit. Atherosclerosis 1995;114:157–64.

25. Lu CH, Lin CH, Li KJ, et al. Intermediate molecular mass hyaluronan and CD44 receptor interactions enhance neutrophil phagocytosis and IL-8 production via p38- and ERK1/2-MAPK signalling pathways. Inflammation 2017;40:1782–93.

26. Butler LM, Rainger GE, Nash GB. A role for the endothelial glycosaminoglycan hyaluronan in neutrophil recruitment by endothelial cells cultured for prolonged periods. Exp Cell Res 2009;315:3433–41.

27. Aruffo A, Stamenkovic I, Melnick M, Underhill CB, Seed B. CD44 is the principal cell surface receptor for hyaluronate. Cell 1990;61:1303–13.

28. Teder P, Vandivier RW, Jiang D, et al. Resolution of lung inflammation by CD44. Science 2002;296:155–8.

29. Salles G, Zain M, Jiang WM, Boussiotis VA, Shipp MA. Alternatively spliced CD44 transcripts in diffuse large-cell lymphomas: characterization and comparison with normal activated B cells and epithelial malignancies. Blood 1993;82:3539–47.

30. Sherman L, Sleeman J, Herrlich P, Ponta H. Hyaluronate receptors: key players in growth, differentiation, migration and tumor progression. Curr Opin Cell Biol 1994;6:726–33.

31. Huebener P, Abou-Khamis T, Zymek P, et al. CD44 is critically involved in infarct healing by regulating the inflammatory and fibrotic response. J Immunol 2008;180:2625–33.

32. Stern R, Asari AA, Sugahara KN. Hyaluronan fragments: an information rich system. Eur J Cell Biol 2006;85:699–715.

33. Bracke KR, Dentener MA, Papakonstantinou E, et al. Enhanced deposition of low-molecular-weight hyaluronan in lungs of cigarette smoke-exposed mice. Am J Respir Cell Mol Biol 2010;42:753–61.

34. Moseley R, Waddington RJ, Embery G. Degradation of glycosaminoglycans by reactive oxygen species derived from stimulated polymorphonuclear leukocytes. Biochim Biophys Acta 1997;1362:221–31.

35. Shirai T, Hilhorst M, Harrison DG, Goronzy JJ, Weyand CM. Macrophages in vascular inflammation: from atherosclerosis to vasculitis. Autoimmunity 2015;48:139–51.

36. Harada H, Takahashi M. J CD44-dependent intracellular and extracellular catabolism of hyaluronic acid by hyaluronidase-1 and -2. Biol Chem 2007;282:5597–607.

37. Kong X, Chen L, Ye P, et al. The role of HYAL2 in LSS-induced glycocalyx impairment and the PKA-mediated decrease in eNOS-Ser-633 phosphorylation and nitric oxide production. Mol Biol Cell 2016;27:3972–9.

38. Bot PT, Pasterkamp G, Goumans MJ, et al. Hyaluronic acid metabolism is increased in unstable plaques. Eur J Clin Invest 2010;40:818–27.

39. Flego D, Severino A, Trotta F, et al. Reduced CD31 expression on CD14(+)CD16(+) monocyte subset in acute coronary syndromes. Int J Cardiol 2015;197:101–4.

40. Flego D, Liuzzo G, Weyand CM, Crea F. Adaptive immunity dysregulation in acute coronary syndromes: from cellular and molecular basis to clinical implications. J Am Coll Cardiol 2016;68:2107–17.

41. Partida RA, Libby P, Crea F, Jang IK. Plaque erosion: a new in vivo diagnosis and a potential major shift in the management of patients with acute coronary syndromes. Eur Heart J 2018;39:2070–6.

KEY WORDS ACS, hyaluronan, inflammation, intact fibrous cap, OCT, personalized medicine

APPENDIX For an expanded Methods section as well as a supplemental table and figures, please see the online version of this paper.